



# Tissue engineering scaffold material of nano-apatite crystals and polyamide composite

Wei Jie, Li Yubao \*

*Research Center for Nano-Biomaterials, Analytical and Testing Center, Sichuan University, Chengdu 610064, China*

Received 12 August 2003; received in revised form 20 October 2003; accepted 20 October 2003

## Abstract

A new kind of tissue engineering scaffold materials of needle-like nano-hydroxyapatite (n-HA) and polyamide (PA) biocomposite is prepared by co-solution, co-precipitation method and water treatment under normal atmospheric pressure. The n-HA crystals uniformly distribute in the composite with a crystal size of 10–20 nm in diameter by 70–90 nm in length. The n-HA/PA composite has good homogeneity, high n-HA content (65 wt%), and high bioactivity. Strong molecule interactions and chemical bondings are present between the n-HA and PA in the composite, which are verified by IR, XPS and XRD. The composite has excellent mechanical properties close to the natural bone. The porous 3-D scaffold is made by injection foaming method, which has not only macropores, but also micropores on the walls of macropores. The porosity is 80% and the average macropore diameter is about 300  $\mu\text{m}$  of the composite. The n-HA/PA composite can be used for tissue engineering and bone repair or substitute.

© 2003 Elsevier Ltd. All rights reserved.

*Keywords:* Nano-apatite; Polyamide; Biocomposite; Tissue engineering; Scaffold material

## 1. Introduction

One of the key technologies in tissue engineering is the preparation of scaffold material for cell culture and tissue repair. Hydroxyapatite (HA) ceramics have been used as tissue engineering material for cell culture and tissue repair due to its biocompatibility and osteoconductivity [1–3]. However, the brittleness and fatigue failure in the body of HA ceramics limit their clinical applications only for unloading bearing repair and substitute [4]. It has been found that each category of bioceramic and polymer cannot fulfill well the demand of bone repair application. Therefore, apatite/polymer biocomposite should be a possible combination of the advantages of the two biomaterials.

In order to enhance HA bioceramic toughness, provide bioactivity for polymer and simulate the structure and composition of natural bone, the use of HA and polymer to prepare inorganic/organic tissue engineering material with excellent properties is highlighted. Various composite systems have been explored as bone substitute materials, including HA reinforced polyethylene, polylactide, collagen and polyactive®, etc. [5–8].

It is known that the higher the HA content in the composite, the better of the composite bioactivity. At present, most HA/polymer composites are prepared by direct mixing HA powder and polymer resin, which cannot make composite with good homogeneity and high HA content [9,10]. In order to synthesize a ceramic/polymer nano-composite with high HA content, new method and materials system should be developed. It is clear that the smaller of HA particles and the higher of HA content in the composite, the better the homogeneity and bioactivity of the composite. Therefore, n-HA and polar polymer (such as polyamide, which can bond with HA) should be selected to make biocomposite with

\* Corresponding author. Tel./fax: +86-288-541-7273.

E-mail addresses: [jiewei7860@sina.com](mailto:jiewei7860@sina.com) (Wei Jie), [nic7504@scu.edu.cn](mailto:nic7504@scu.edu.cn) (Li Yubao).

high HA content and good mechanical strength for tissue engineering. Polyamide has good biocompatibility with human tissue, probably due to its similarity to collagen protein in chemical structure and active groups [11]. In this study, a new method of co-solution, co-precipitation and water treatment under normal atmospheric pressure is employed to prepare n-HA/PA66 composite.

## 2. Materials and methods

164 g calcium nitrate ( $\text{Ca}(\text{NO}_3)_2$ ) was dissolved in 1500 ml *N,N*-dimethyl acetamide (DMAC) in a three-neck flask at 60 °C, then the temperature increased to 140 °C. Fifty five grams PA66 with a viscosity-average molecular weight (*M<sub>v</sub>*) of 18 kDa, was added into the three-neck flask, keeping the temperature at 140 °C for 4 h till PA66 was dissolved completely, thus the co-solution of calcium nitrate, PA66 and DMAC was obtained. 98.4 g sodium phosphate ( $\text{Na}_3\text{PO}_4$ ) was dissolved in aqueous solution, the co-solution was dropped slowly into the sodium phosphate aqueous solution with stirring at room temperature, pH value was adjusted to 10 by adding sodium hydroxide. When the reaction ended, the co-precipitation mixture was set 24 h at room temperature. After fully washed by deionized water four times and ethanol twice, the obtained n-HA/PA66 composite product was put into flask to treat in deionized water for 4 h at 90–100 °C under normal atmospheric pressure, then cooled down to room temperature, dried in a vacuum oven at 50–80 °C for 48 h. n-HA/PA66 composite samples were made with an injection moulding machine. Porous n-HA/PA66 composite samples were made by injection foaming method with the same injection moulding machine. A foam agent of barium azodicarboxylate was used. The injection temperature ranged from 260 to 290 °C under 15 MPa pressure.

n-HA was prepared by following procedure:

164 g  $\text{Ca}(\text{NO}_3)_2$  aqueous solution was dropped into 98.4 g  $\text{Na}_3\text{PO}_4$  aqueous solution with stirring, the pH value was also adjusted to 10 by adding sodium hydroxide. After the titration was finished, the mixture set at room temperature for 24 h at room temperature.

The obtained apatite precipitate was washed with deionized water for four times and put into flask to treat in deionized water for 4 h at 90–100 °C under normal atmospheric pressure. After treatment, the apatite precipitate became n-HA, then dried at 80 °C, n-HA powder was obtained.

The calcium nitrate, sodium phosphate and DMAC are from Chengdu Chemical Agent Co. Ltd., China, AR grade. PA66 is from Asahi Chemical Industry Co. Ltd., Japan. Transmission electron microscopy (TEM, JEM-100CX) was employed to test the size of n-HA with powders and the composite particles with powders. X-ray diffraction (XRD, Philips XRD analyzer) was used to detect the phase composition and crystallinity of the composite powders and n-HA powders. Fourier transform infrared absorption spectra (FT-IR, Nicolet 170SX) and X-ray photo-electronic spectroscopy (XPS, XSAM 800) were used to determine the chemical bondings between n-HA and PA66 of the composite powders. Tensile strength, bending strength, compressive strength and elastic modulus of the composite dense sample made by injection were determined by universal material test machine with the average values of four specimens. The macropore diameter and morphology of the porous composite were observed by scanning electron microscopy (SEM, JEOL JSM5600LV). Mercury intrusion porosimetry (Porous Materials Inc., NY) was used to determine the porosity of the scaffolds with the average values of two specimens. n-HA content in the composite with the average values of three specimens was tested by burning the composite at 800 °C under air atmosphere.

## 3. Results

### 3.1. n-HA content in composite

Table 1 is the n-HA content in the composite tested by burning the composite at 800 °C under air atmosphere. The data shows that the n-HA content in different parts of the same the sample is almost the same. This indicates that the composite with good homogeneity and expected n-HA content (upto 65 wt%) in the

Table 1  
n-HA content in composite and mechanical properties of dense composite sample (mean  $\pm$  standard deviation) ( $n = 3$  for n-HA content;  $n = 4$  for mechanical properties)

Sample	n-HA content (%)	Tensile strength (MPa)	Bending strength (MPa)	Compressive strength (MPa)	Elastic modulus (GPa)
1	38.71 $\pm$ 0.208	65 $\pm$ 4	77 $\pm$ 5.0	93 $\pm$ 7.1	3.6 $\pm$ 0.3
2	45.06 $\pm$ 0.012	71 $\pm$ 1	85 $\pm$ 2.3	106 $\pm$ 2.6	4.0 $\pm$ 0.5
3	51.78 $\pm$ 0.252	74 $\pm$ 3	87 $\pm$ 3.6	112 $\pm$ 6.0	4.9 $\pm$ 0.2
4	64.25 $\pm$ 0.270	87 $\pm$ 2	95 $\pm$ 5.2	117 $\pm$ 4.1	5.6 $\pm$ 0.3

composite can be obtained through this synthesized method.

### 3.2. Mechanical properties of composite

The composite has good mechanical properties. The bending strength, tensile strength, compressive strength and elastic modulus of the composite sample are shown in Table 1.

### 3.3. IR and XPS analysis

The IR spectrum of n-HA is shown in Fig. 1a. It can be seen that the absorption peaks at 3571 and 632  $\text{cm}^{-1}$ , representing bending vibration of hydroxyl ( $-\text{OH}^-$ ), obviously decrease in composite as shown in Fig. 1c. The peaks in Fig. 1a at 566, 1034 and 1095  $\text{cm}^{-1}$  belonging to  $\text{PO}_4^{3-}$  in n-HA, move to 568, 1037 and 1092  $\text{cm}^{-1}$  in the composite. Bands around 2924 and 2851  $\text{cm}^{-1}$  represent carbon hydrogen ( $-\text{CH}_2-$ ) vibration, the two peaks move to 2931 and 2858  $\text{cm}^{-1}$  in composite as shown in Fig. 1c. The band around 1544  $\text{cm}^{-1}$  representing the stretching vibrations of carbon–nitrogen (C–N) and hydrogen–nitrogen (H–N) of PA in Fig. 1b moves to 1537  $\text{cm}^{-1}$  in composite. The characteristic adsorption peak at 3300  $\text{cm}^{-1}$  in Fig. 1b for nitrogen hydrogen ( $-\text{NH}-$ ) vibration of PA moves to 3313  $\text{cm}^{-1}$  in composite. The band around 1640  $\text{cm}^{-1}$  for the carbonyl ( $-\text{C}=\text{O}$ ) vibration of PA displaces to 1636  $\text{cm}^{-1}$  in composite. A new peak appears at 1417  $\text{cm}^{-1}$  for carboxyl ( $-\text{COO}^-$ ) stretching vibration in the composite [12–14].

Fig. 2 is the XPS curve of n-HA/PA composite and n-HA. The binding energy of calcium atom (Ca), phosphorous atom (P) and oxygen atom (O) has some difference between n-HA (O: 531.2, Ca: 351.5 and 347.5, P: 134.5 eV) and the composite (O: 531.6, Ca: 351.8 and 348.2, P: 135.4 eV). The binding energy of O in the composite is higher than that of n-HA by 0.4, Ca by 0.3 and 0.7, and P by 0.9 eV respectively. This means that

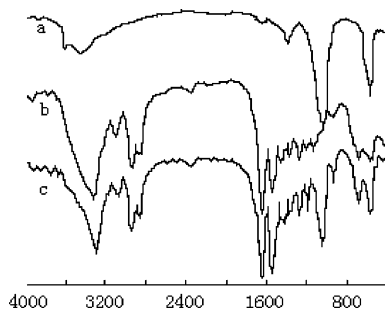


Fig. 1. IR spectra of n-HA (a), PA66 (b) and n-HA/PA66 composite (c).

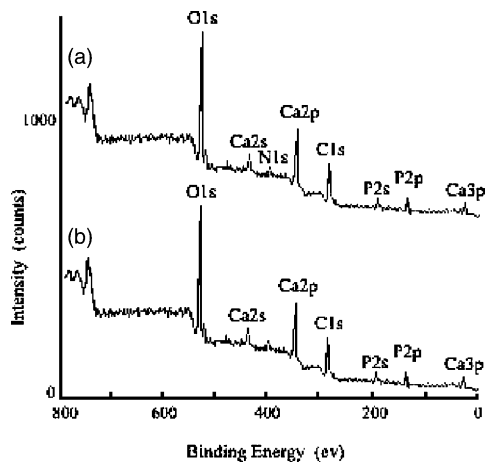


Fig. 2. XPS curve of n-HA/PA66 composite (a) and n-HA (b).

the binding energy of Ca, O and P increases in the composite.

### 3.4. XRD analysis

Fig. 3 shows relevant XRD patterns, in which 3a is PA66, 3b is n-HA/PA66 composite and 3c is n-HA. The PA66 in Fig. 3a and b have two characteristic peaks at  $2\theta = 20^\circ$  and  $24^\circ$  [15]. It can be obtained from 3a and 3b that the crystallinity of PA66 and PA66 in the composite is 35% and 24% respectively. The results show that the crystallinity of PA66 decreased in the composite, indicating that the crystal structure of PA66 changed after forming composite with n-HA. The crystalline peaks of n-HA at  $2\theta = 25.9^\circ, 32^\circ, 33^\circ, 34^\circ, 35.5^\circ$  and  $40^\circ$  are shown in Fig. 3b and c, exhibiting a HA structure. The n-HA and n-HA in composite belong to a poorly crystallized apatite structure as shown in Fig. 3b and c.

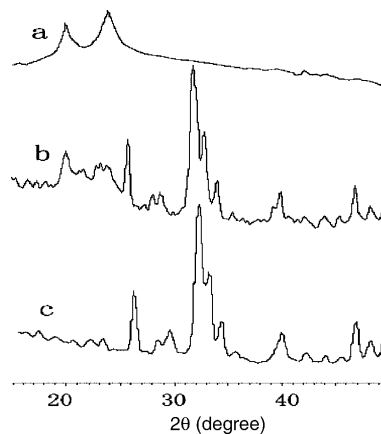


Fig. 3. XRD spectra of PA66 (a), n-HA/PA66 composite (b), n-HA (c).

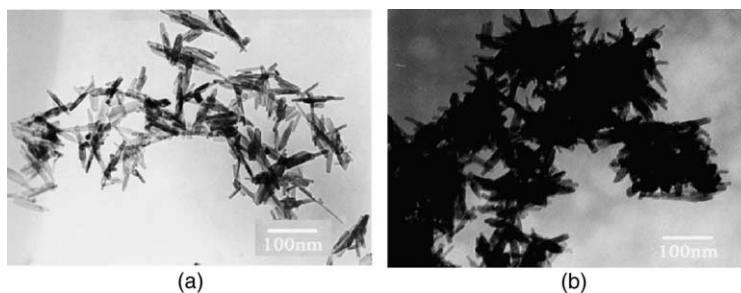


Fig. 4. TEM photographs of n-HA crystals (a) and n-HA/PA66 composite (b).

From the XRD patterns, it can be calculated by Scherrer equation that the mean size of n-HA crystals and n-HA crystals in composite is about 20 nm in diameter by 75 nm in length.

### 3.5. TEM analysis

The TEM photographs of n-HA crystals (a) and n-HA/PA66 composite (b) are shown in Fig. 4. The size of n-HA crystals and n-HA crystals in composite is about 10–20 nm in diameter by 70–90 nm in length as shown in Fig. 4. The needle-like n-HA crystals distribute in PA66 matrix and combine closely with the PA66.

### 3.6. Porosity and pore diameter of composite

The photographs of the three-dimension (3-D) porous n-HA/PA66 composite scaffold materials are shown in Fig. 5. The SEM photographs of the porous composite are shown in Fig. 6. The results indicate that the porous composite has not only macropores, but also a lot of micropores on the walls of macropores, and the



Fig. 5. Photographs of porous n-HA/PA66 scaffold materials.

pores are interconnected. The macropores diameter of the scaffold material is from 100 to 500  $\mu\text{m}$ , the mean diameter is about 300  $\mu\text{m}$ . The porosity, open and close pores percentages of the porous composite scaffold with different n-HA content in the composites are shown in Table 2. The porosity and close pores percentages of the porous scaffold increase with the rise of the n-HA content in the composite.

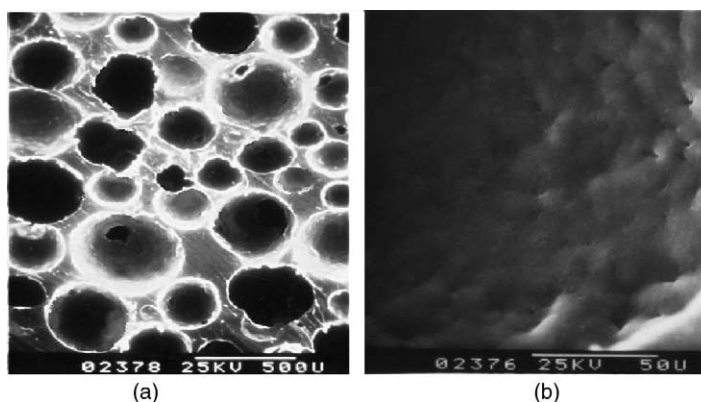


Fig. 6. SEM photographs of the porous n-HA/PA66 composite, the macropores material (a) and the micropores on macropores' walls (b).

Table 2

Porosities, close and open pores percentages of composite scaffold with different n-HA content (mean  $\pm$  standard deviation) ( $n = 2$  for porosity, close and open pores percentages)

Sample	n-HA content (%)	Porosity (%)	Close pore (%)	Open pore (%)
1	38.71	71 $\pm$ 5	9 $\pm$ 1	91 $\pm$ 5
2	45.06	76 $\pm$ 2	12 $\pm$ 2	87 $\pm$ 5
3	51.78	77 $\pm$ 3	17 $\pm$ 1	85 $\pm$ 5
4	64.25	80 $\pm$ 2	19 $\pm$ 3	81 $\pm$ 5

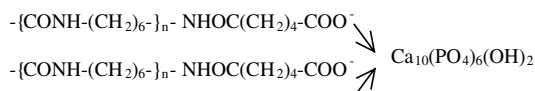
#### 4. Discussion

HA has an inorganic component similar to that in human hard tissue. It has a good biocompatibility and can bond to bone tissue in body. The outstanding biological performance of HA biomaterial has been widely proved in the forms of bone filler, coating on titanium alloy, and recently as scaffolds for cell carrier in bone tissue engineering. The use of scaffold material in bone tissue engineering is to either induce formation of bone from surrounding tissues or to act as a carrier or template for bone cells or other agents. Porous scaffold can allow bone growth into its construct [16–19]. In this study, a novel method of co-solution, co-precipitation and water treatment under normal atmospheric pressure was employed to make biomaterial of n-HA/PA66 composite, and porous scaffold materials were prepared by injection foaming method. The porous n-HA/PA66 scaffold can provide advantages for bone tissue engineering: (a) a better environment is expected for cell seeding, survival, growth and differentiated function because of the osteoconductive properties imparted by n-HA; (b) the mechanical properties can be improved greatly; (c) the porous scaffold can guide cell attachment, migration, proliferation, differentiation, and tissue regeneration in 3-D structure.

To achieve the desired bioactivity, it is necessary to improve n-HA content in composite. Conventional melting method by mechanically mixing HA powders with polymer to prepare HA/polymer composite is difficult to ensure high HA content in composite with good homogeneity [20,21]. The burning test indicates that the n-HA content in different parts of the same sample is almost same, this means that the prepared composite with high n-HA content has a good homogeneity. The new method of co-solution, co-precipitation and water treatment used in this experiment is more helpful to make n-HA/polymer composite than mechanically mixing with clogged powders under high temperature or/and high pressure.

In making n-HA/polymer composite with good mechanical properties, the interface between the inorganic mineral and organic polymer should be first optimized to create proper chemical bondings between the two phases. Polyamide is a polymer with polar

groups in its molecular chain. The polar polymer has relatively high affinity to polar fillers (e.g. n-HA) [22]. IR analysis shows that some adsorption peaks of the n-HA and PA66 have variations in the composite: the  $\text{PO}_4^{3-}$  peaks of the n-HA at 566, 1034 and 1095  $\text{cm}^{-1}$ , move to 568, 1037 and 1092  $\text{cm}^{-1}$  in the composite;  $-\text{CH}_2-$  vibration peaks at 2924 and 2851  $\text{cm}^{-1}$  move to 2931 and 2858  $\text{cm}^{-1}$ , respectively, The PA66 stretching vibration peaks of  $-\text{CN}-$  and  $-\text{HN}-$  at 1544 move to 1537  $\text{cm}^{-1}$ . These results indicate that some molecule interactions may be present between the n-HA and PA66 in the composite. The  $-\text{OH}-$  absorption peaks at 3571 and 632  $\text{cm}^{-1}$  of n-HA obviously decrease in the composite. The  $-\text{NH}-$  characteristic adsorption peak of PA at 3300 shifts to 3313  $\text{cm}^{-1}$ , the  $-\text{C}=\text{O}$  vibration peak of PA at 1640 displaces to 1636  $\text{cm}^{-1}$  in the composite. These results mean that hydrogen bonding may be formed between the  $-\text{OH}-$  group of n-HA and  $-\text{C}=\text{O}$  and/or  $-\text{NH}-$  groups of PA66. A new peak for  $-\text{COO}-$  stretching vibration appears at 1417  $\text{cm}^{-1}$  in the composite, which may result in the  $-\text{COO}-$  group of PA66 bonding with the calcium ion of n-HA. Therefore, it could be deduced that n-HA maybe linked with PA66 by hydrogen bonding and by the formation of carboxyl–calcium–carboxyl linkage as following:



These linkages have strong effect on interface behavior and mechanical properties of the composite.

The crystallinity of PA66 decreases in composite, the hydrogen bonds in PA66 contribute to its crystallinity, indicating that the crystallized structure of PA66 changed after forming composite with n-HA. In the composite, the appeared interface bonding between the n-HA and PA66 may result in the number decrease of hydrogen bonds of PA66, thus lessens the crystallinity of PA66.

XPS shows that the binding energy of calcium atom, phosphorous atom and oxygen atom of n-HA has some change in the composite. The results also indicate that chemical bondings are present between the n-HA and

PA66. Combining the IR, XRD and XPS analysis, it can be drawn a conclusion that strong molecule interactions and chemical bondings are present between the n-HA and PA66 interface in the composite.

Chemical bonding and strong molecule interaction between n-HA and PA66 obviously affect the mechanical properties of the composite, making the composite have good mechanical strength. The bending strength, tensile strength and compressive strength of the composite with 64.25 wt% n-HA content are 95, 79 and 117 MPa, respectively, which is close to the natural bone (80–100, 60–120, 50–140 MPa separately [23]). The elastic modulus of the composite prepared in this study is 5.6 GPa, while the elastic modulus of bioceramics and medical metals is much higher (70–300 GPa) than the natural bone (3–25 GPa) and thus cause stress stimulating or shielding effect, which often result in bone resorption and loosening of implants [24,25]. Therefore, the composite prepared in this study can match well to that of human bone. The results show that the use of n-HA crystals can not only increase bioactive HA content in the composite but also ensure the biomechanical properties. The good mechanical properties of the n-HA/PA66 composite also result from n-HA particle size and surface activity, this makes it possible for n-HA to link with polyamide more strongly.

The composite can be processed into 3-D interconnected porous structure. The porous scaffold material not only has macropores but also possesses micropores, which could allow a fast bone ingrowth and a good osteointegration. The micropores in the macropores surface could enlarge greatly the surface area for protein adsorption, more protein absorbed on pore surface and the easier to facilitate bone formation. The rough surface and pore walls can enhance osteogenic precursor cell adhesion, proliferation and differentiation [26].

The porosity of the scaffold is very important, because it can affect the growth and migration of the planting cell. The higher the n-HA content, the higher the porosity of the porous scaffold, which is because the porous composite scaffolds with low n-HA content have high shrinkage after the composite samples were made by injection foaming method. The porosity of the porous n-HA/PA66 scaffold is 80% with 64.25% n-HA content in composite, which can enable the circulation of physiological fluid to provide nutrients for tissue and cells [27]. The porous size and inner surface area is important for the growth of the bone tissue into the scaffold, the bigger inner surface area, the more the planting cells in it, and the faster the tissue and organ formation [28]. The n-HA content in the composite also affect the pore characteristics, the higher the n-HA content, the higher the close pores percentage of the porous scaffold, which is because the composite with high n-HA content have low shrinkage. The shrinkage of the composite made by injection foaming affects not

only the porosity but also close pores and micropores of the porous scaffold. The macropores diameter of the scaffold is from 100 to 500  $\mu\text{m}$ , which is very suitable for tissue ingrowth and nourishment substance transportation. The use of injection foaming method could be a promising way to obtain scaffold materials with interconnected macropores and micropores.

## 5. Conclusion

Tissue engineering scaffold material of n-HA/PA66 composite prepared by co-solution co-precipitation method has not only good homogeneity but also high HA contents. Interface chemical bondings are present between the n-HA and PA66 in the composite. The composite has excellent mechanical properties close to that of natural bone. The porous material has not only macropores but also micropores on the walls of the macropores. Such biomaterial with well-controlled composition and porous structure can be a good bone repair materials and can provide a standard scaffold for investigating the cell/material interaction in tissue engineering.

## Acknowledgements

The financial support from the Ministry of Science and Technology of China and the Ministry of Education of China are gratefully acknowledged.

## References

- [1] Hardy DCR, Frayssinet P. Osteointegration of hydroxyapatite coated stems of femoral prostheses. *Eur J Orthop Surg Traumatol* 1999;9:75–81.
- [2] Gazdag A, Lane J, Glaser D, Forster R. Alternatives to autogenous bone graft: efficacy and indications. *J Am Acad Orthop Surg* 1995;3:1.
- [3] Maxian SH, Zawadsky JP, Dunn MG. In vitro evaluation of amorphous calcium phosphate and poorly crystallized hydroxyapatite coatings on titanium implants. *J Biomed Mater Res* 1993;27:111–7.
- [4] Cleries L, Fernandez Pradas JM, Morenza JL. Behavior in simulated body fluid of calcium phosphate coatings obtained by laser ablation. *Biomaterials* 2000;21:1861–5.
- [5] Du C, Cui FZ, Feng QL, Zhu XD, de Groot K. Tissue response to nano-hydroxyapatite/collagen composite implants in marrow cavity. *J Biomed Mater Res* 1998;42:540–8.
- [6] Zhang RY, Ma PX. Porous poly(L-lactic acid)/apatite composites created by biomimetic process. *J Biomed Mater Res* 1999;45:285–93.
- [7] Bonfield W, Grynblas MD, Tully AE, Bowman J, Abram J. Hydroxyapatite reinforced polyethylene—a mechanically

- compatible implant material for bone replacement. *Biomaterials* 1981;2:185–6.
- [8] Du C, Meijier GJ, van de Valk C, Haan RE, Bezemer JM, Hessling SC, et al. Bone growth in biomimetic apatite coated porous Polyactive® 1000 PEGT70PBT30 implants. *Biomaterials* 2002;23:4649–56.
- [9] Di Silvio L, Dalby M, Bonfield W. In vivo response of osteoblasts to hydroxyapatite-reinforced polyethylene composites. *J Mater Sci Mater Med* 1998;9:845–8.
- [10] Shikinami Y, Okuno M. Bioresorbable devices made of forged composites of hydroxyapatite (HA) particles and poly(L-lactide) (PLLA). Part II: practical properties of mini-screws and miniplates. *Biomaterials* 2001;22(23):3197–211.
- [11] Wang X, Li Y, Wei J. *Chin J Biomed Eng* 2001;10:199–203.
- [12] Guo Y, Li Y, Yan G. Preparation and interface properties of nanoapatite crystals/polyamide66. *J Sichuan University (Science edition)* 2002;3:480–3.
- [13] Wang X, Li Y, Wei J. Development of biomimetic nano-hydroxyapatite/poly(hexamethylene adipamide) composites. *Biomaterials* 2002;23:4787–91.
- [14] Wei J, Li Y. Injectable premixed cement of nanoapatite and polyamide composite. *High Technol Lett* 2002;2:18–22.
- [15] Wang X, Li Y. A study on nanoapatite crystals and polamide biomimetic composite. *High Technol Lett* 2002; 2:18–22.
- [16] Browne M, Gregson PJ. Effect of mechanical surface pretreatment on metal ion release. *Biomaterials* 2000;21:385–92.
- [17] Zeng H, Chittur KK, Laceeld WR. Dissolution/precipitation of calcium phosphate thin films produced by ion beam sputter deposition technique. *Biomaterials* 1999;20: 443–51.
- [18] Zhang Y, Zhang M. Synthesis and characterization of macroporous chitosan/calcium phosphate composite scaffolds for tissue engineering. *J Biomed Mater Res* 2001; 26:304–12.
- [19] Redey SA, Nardin M, Bernache-Assolant D, Rey C, Delannoy P, Sedel L, et al. Behavior of human osteoblastic cells on stoichiometric hydroxyapatite and type A carbonate apatite: role of surface energy. *J Biomed Mater Res* 2000;50:353–64.
- [20] Bonfield W, Wang M, Tanner KE. Interfaces in analogue biomaterials. *Acta Mater* 1998;46:2509–18.
- [21] Ramakrishna S, Mayer J, Wintermantel E, Kam Leong W. Biomedical applications of polymer-composite materials: a review. *Compos Sci Technol* 2000;61:1189–224.
- [22] Yan Y, Li Y. Synthesis and properties of a copolymer of poly(1,4-phenylene sulfide)–poly(2,4-phenylene sulfide acid) and its HA reinforced composite. *Eur Polym J* 2003;2: 411–6.
- [23] Verheyen CCPM, de Wijn JK, van Blitterswijk CA. Evaluation of hydroxyapatite/poly(L-lactide) composites: mechanical behavior. *J Biomed Mater Res* 1992;26:1277–96.
- [24] Peppas NA, Langer R. New challenges in biomaterials. *Science* 1994;263:1715–20.
- [25] Damien CJ, Parson JR. Bone graft and bone graft substitutes: a review of current technology and applications. *J Appl Biomater* 1992;2:187–208.
- [26] Burg KJL, Porter S, Kellam JF. Biomaterial developments for bone tissue engineering. *Biomaterials* 2000;21:2347–59.
- [27] Mooney DJ, Baldwin DF, Suh NP. Novel approach to fabricate porous spongers of poly(DL-lactic-co-glycolic acid) without the use of organic solvents. *Biomaterials* 1996;14:1417–22.
- [28] Koller MR, Palsson MA, Manchel I. Tissue culture surface characteristics influence the expansion of human bone marrow cells. *Biomaterials* 1998;19:1963–72.